FUDMA Journal of Sciences (FJS)
ISSN online: 2616-1370
ISSN print: 2645 - 2944
Vol. 10 No. 10, May, 2026, pp 208 – 214
DOI: https://doi.org/10.33003/fjs-2026-1010-5184

Hematological and Serum Protein Profiles in a Wistar Rat Model of Severe Protein-Energy Malnutrition Induced by a LOW-Protein, High-Carbohydrate Diet

***[1]Amira Esther O., [2]Vining-Ogu Ibukun C, [1]Hassan Rihanat I, [1]Salaudeen Kafayat A., [1]Abdulrahman-Orire Rofiat. A., [1]Alli Abdulhameed O., [1]Gana Esther O, [1]Kudabo Samuel A.**

[1]Department of Science Laboratory Technology, Kwara State Polytechnic, Ilorin, Kwara State, Nigeria.
[2]Department of Science Laboratory Technology, Biochemistry Unit, Akanu Ibiam Federal Polytechnic, Unwana, Afikpo, Ebonyi State, Nigeria.

*Corresponding authors' email: amiraesther36@gmail.com

ABSTRACT

This study evaluated the physiological, biochemical, and hematological impacts of severe protein restriction using an approximated animal model of protein-energy malnutrition (PEM). Ten young male Wistar rats were divided into a control group fed standard commercial chow *(n=5)* and an experimental group fed a formulated protein-depleted diet (*n=5*; 3.47% protein, 81.53% carbohydrate) for an extended period of 42 days. The diet was designed based on the historical threshold established by Boyd et. al. (1968), which demonstrates that dietary protein must remain at or below 3.47% to replicate clinical, kwashiorkor-like pathology in rodents.

By the conclusion of the feeding trial, severe dietary protein deficiency induced an immediate, progressive loss of body mass, with the experimental cohort dropping from an initial 60.58 ± 10.35g to a final 38.66 ± 5.23g *($p < 0.05$)*. This structural decline was accompanied by behavioral lethargy, extensive alopecia, and visible muscle wasting. Biochemical analysis revealed severe hypoproteinemia, with total plasma protein falling from 3.5 ± 0.66g/dL in controls to 1.64 ± 0.55g/dL in the malnourished group *($p < 0.05$)*, driven by a deep drop in serum albumin (1.0 ± 0.3g/dL) and globulin (0.64 ± 0.26g/dL) fractions. Manual hematological profiles showed severe nutritional anemia, with hemoglobin and hematocrit cut nearly in half, alongside profound leukopenia and lymphopenia *($p < 0.05$)*. While the compact sample size limits broad generalizability, these findings offer a synchronized baseline of the metabolic, erythroid, and immune collapse that approximates advanced clinical malnutrition, serving as an accessible experimental paradigm for evaluating targeted nutritional interventions.

Keywords: Protein-Energy Malnutrition, Wistar Rats, Boyd Threshold, Hypoproteinemia, Nutritional Anemia, Leukopenia

INTRODUCTION

Protein-energy malnutrition (PEM) remains one of the most pressing public health challenges across developing nations, contributing significantly to high morbidity and mortality rates, particularly among vulnerable pediatric populations. Clinically manifested as marasmus, kwashiorkor, or intermediate marasmic-kwashiorkor states, PEM is rarely a product of simple, isolated starvation. Instead, it frequently arises from an insidious dietary imbalance: a severe deficit in quality protein alongside a high or sustained intake of cheap, starchy carbohydrates (Müller & Krawinkel, 2005). While the macro-level physical consequences of this condition—such as wasting and stunted growth—are easily visible, the internal, progressive systemic breakdown of immune defense mechanisms and blood homeostasis requires deeper biochemical investigation.

A primary obstacle in managing and treating severe malnutrition is the complexity of capturing its early-to-moderate metabolic shifts before irreversible multi-organ failure sets in. While clinical studies on malnourished children provide invaluable endpoint data, they are frequently confounded by secondary infections, varying genetic backgrounds, and unreliable dietary histories (Waterlow, 1984). Consequently, controlled animal models are essential for mapping the precise, unconfounded timeline of metabolic degradation. A foundational benchmark in establishing these models was achieved by Boyd et. al. (1968), who demonstrated that the classic, clinical kwashiorkor-like syndrome cannot be successfully replicated in albino rats if the dietary protein level exceeds 3.47%.

While various low-protein rodent models exist extensively within contemporary literature, many setups utilize absolute starvation or zero-protein diets, which fail to accurately mirror real-world human sub-nutrition where carbohydrates are still consumed. Simulating this exact nutritional disparity in experimental rodent designs is essential to understanding the localized tissue wasting and shifts in blood morphology that occurs during prolonged human undernutrition. Furthermore, historical data from clinical kwashiorkor cases has shown a distinct asymmetry in hepatic responses, noting a severe drop in plasma albumin synthesis but an enigmatic preservation or lack of change in gamma-globulin levels under certain conditions.

While absolute fasting models provide insight into total starvation dynamics, they fail to replicate the complex metabolic adaptations seen in human public health crises. In real-world settings, clinical conditions like kwashiorkor and marasmic-kwashiorkor do not arise from total food deprivation, but rather from a chronic dietary imbalance where an extreme deficit in quality protein is masked by a high intake of cheap, starchy carbohydrates. Establishing a precise, validated macronutrient baseline becomes vital for separating the systemic effects of true protein deficiency from generalized caloric starvation (Mhlomi, Unuofin, et. al., 2022).

This study addresses the critical need to validate these historical, structural thresholds against the sophisticated diagnostic matrices available in modern hematology and serum biochemistry. While previous literature has extensively documented individual pieces of the malnutrition puzzle—such as fluid imbalances or basic weight loss—there remains a continuous need for integrated data evaluating how a strict, Boyd-threshold diet simultaneously impairs erythropoiesis, cellular immunity, and specific serum protein fractions over a

fixed chronological window. Furthermore, a primary challenge in custom low-protein formulations is the confounding effect of generalized micronutrient deficiencies. To isolate severe protein restriction as the sole experimental variable, the custom dietary architecture must explicitly include comprehensive vitamin and mineral supplementation, thereby mitigating potential micronutrient adequacy confounders.

The primary aim of this work is to systematically evaluate the impact of a targeted, protein-deficient diet (3.47% protein, 81.53% carbohydrate) on the complete biochemical and hematological profiles of Wistar rats over a 42day period. This research contributes incremental value to the current body of knowledge by providing a highly synchronized, multi-parameter physiological profile that bridges macro-morphological changes (such as muscle wasting and alopecia) directly with internal cellular decline. By doing so, it offers a definitive reaffirmation of the 3.47% protein threshold as a highly reliable tool for studying the progressive, moderate-to-severe stages of human malnutrition approximation, ultimately aiding in the refinement of targeted therapeutic and dietary interventions.

MATERIALS AND METHODS

Experimental Animals and Environment

Healthy, young male albino Wistar rats (initial body weight approximately 60 - 62g) were obtained from the animal house of the Kwara State Polytechnic, Ilorin, Nigeria. The animals were housed in clean, well-ventilated plastic cages under standard laboratory conditions, maintaining a regular 12-hour light/dark cycle and room temperature (25 ± 2^{o}C). All animals were allowed a 7-day acclimatization period, during which they had free access to standard commercial rodent chow and clean drinking water *ad libitum.*

Formulations of the Experimental Diets

Two distinct dietary regimens were utilized in this study. The control diet consisted of standard, commercially balanced Purina rodent chow. Concurrently, a custom kwashiorkor genic, protein-depleted diet was prepared by modifying the foundational diet models of Boyd and Carsky (1969). The diet was structured to contain all required vital nutrients in a definite, localized proportion.

To isolate protein deficiency as the single independent variable while ensuring micronutrient adequacy, the ingredients were sourced and integrated as follows:

Carbohydrate Matrix

Locally processed Garri (cassava granules) was utilized as the primary carbohydrate base.

Protein Source

Ground soybean was incorporated in a strictly limited proportion to serve as the minimal dietary protein source.

Dietary Fat

Refined vegetable oil purchased from a local commercial market served as the lipid component.

Vitamin & Trace Mineral Supplements

Sourced in the form of growers' macromix from Adom Feed Mill (Ibadan, Nigeria), utilizing the benchmark mixture originally formulated by Glaxo Laboratories and reported by Cuthbertson (1957).

Mineral Salts Matrix

Composed of bone meal (calcium phosphate), oyster shell (tri-potassium citrate), and pure sodium chloride, procured from Adom Feed Mill (Ibadan, Nigeria) based on the structural salt balances described by Rippon (1959).

The precise percentage macronutrient profile and the chemical concentrations per kilogram of the dietary formulations are comprehensively detailed below in Tables 1, 2, and 3. This specific matrix was selected because Boyd et al. (1968b) established that if the level of dietary protein exceeds 3.47%, a clinical kwashiorkor-like syndrome cannot be successfully approximated in albino rats.

Table 1: Macronutrient Composition of the Protein-Depleted Experimental Diet

Nutrients	% Composition
Carbohydrate (Garri)	81.53
Protein (Soybean)	3.47
Vitamin Supplement (Growers Macromix)	3.00
Mineral Supplement	4.00
Vegetable Oil	8.00

Table 2: Composition of Vitamin and Trace Minerals Supplements (Cuthbertson, 1957)

Vitamin/Trace Minerals	Amount per kg Diet
vitamin A(retinol)	4,000,000 I.U
vitamin D3	880,000 I.U
vitamin B1	0.2g
vitamin B2	1.8g
vitamin B_6	1.2g
Nicotinic acid	8.8
Calcium pantothenate	3.2g
Vitamin B_{12}	4.8mg
Choline chloride	80g
manganese	40g
Zinc	18g
Copper	0.8g
Iodine	0.62g
Iron	20g
Cobalt	0.09g

Vitamin/Trace Minerals	Amount per kg Diet
Selenium	0.04g

Table 3: Composition of the Mineral Supplement Matrix (Rippon, 1959)

Salt Matrix	Amount (grams)
Sodium Chloride	22.0
Calcium Phosphate (Bone Meal)	130.0
Tri-Potassium Citrate (Oyster Shell)	125.0
Magnesium Sulphate	30.0

Experimental Design, Randomization, and Animal Monitoring

Following the acclimatization window, the ten Wistar rats were assigned to one of two experimental groups with five rats per group *(n=5)*. To eliminate allocation bias, a simple randomization technique was performed via a computer-generated random number sequence.

Group I (Control Group)

Maintained on the standard commercial chow for the duration of the study.

Group II (Malnourished Group)

Maintained on the formulated 3.47% protein-depleted experimental diet.

Both cohorts had unrestricted, *ad libitum* access to their respective diets and clean drinking water. The feeding trial was extended across a 42day chronological window to observe advanced systemic degradation. Body weight variations (gain and loss dynamics) were systematically tracked at regular 7-day intervals using a calibrated digital laboratory balance. Concurrently, macro-morphological variations, behavior, and physical features—specifically changes in the quality of the fur, paws, facial architecture, and active motor patterns—were monitored and recorded daily by comparing the control and experimental cohorts.

Blood Sample Processing

At the conclusion of the 42 day experimental trial, the animals were weighed and subjected to an overnight fast. The animals were humanely sacrificed under surgical anesthesia using chloroform vapor. Whole blood was immediately collected from both experimental cohorts.

A portion of the harvested blood was collected into tubes containing ethylenediaminetetraacetic acid (EDTA) as an anticoagulant to preserve cellular morphology for manual hematological evaluation. A second portion was channeled into non-coagulant plain tubes, allowed to clot completely at room temperature, and centrifuged at 3000 rpm for 15 minutes to separate the serum. The isolated serum was stored at -20^{o}C for downstream protein assays. To preserve analytical integrity, all sample tubes were blind-coded with arbitrary numerical identifiers, ensuring the laboratory investigators remained blinded to the experimental groupings during downstream testing.

Serum Biochemical Analysis

Total plasma protein and serum albumin concentrations were determined quantitatively utilizing an automated enzymatic colorimetric analyzer manufactured by Randox Daytona. The serum globulin fraction for each animal was calculated mathematically using the direct subtraction formula:

Globulin (g/dL) = Total Protein (g/dL) - Albumin (g/dL)

Manual Hematological Parameters Determination

Hemoglobin (Hb) Concentration (Cyanomethaemoglobin Method)

Blood hemoglobin concentration was determined colorimetrically using the Drabkin's method described by Schalm et al. (1975). The operational principle relies on the biochemical conversion of hemoglobin to methaemoglobin by the action of potassium ferricyanide, which is sequentially converted to stable cyanomethaemoglobin by potassium cyanide.

The Drabkin's reagent was prepared by dissolving 0.2g potassium cyanide, 0.2g potassium ferricyanide, and 1.0 g sodium bicarbonate in 1000 mL of distilled water. For the assay procedure, 0.02 mL of whole blood was mixed into 5 mL of the prepared Drabkin's solution and allowed to stand undisturbed for 10 minutes to guarantee full color development. The absorbance of the test sample and a standard solution of cyanomethaemoglobin were read spectrophotometrically against a blank containing pure Drabkin's solution to compensate for the natural yellow tint of the reagent. The final concentration of hemoglobin was calculated using the formula:

$$\text{Concentration of Hb (g/dL)} = \frac{\text{Colorimetric reading of test}}{\text{Colorimetric reading of standard}} \text{ X Concentration of standard solution}$$

Packed Cell Volume (PCV) (Wintrobe Macro method)

Packed cell volume was determined via the standard Wintrobe hematocrit technique (Schalm et al., 1975). Whole EDTA-anticoagulated blood was thoroughly mixed by inverting the collection tube exactly 20 times. Using a fine-tipped capillary pipette, a Wintrobe hematocrit tube was carefully filled up to the 10 mark, ensuring the complete absence of air bubbles. The filled tube was centrifuged at 3000 rpm for exactly 30 minutes. Following centrifugation, the tube was removed, and the vertical height of the compacted red blood cell column was noted against the 100 uniform divisions on the tube. The final PCV value was read directly off the column scale and expressed as a volumetric fraction of whole blood.

Total White Blood Cell (WBC) Count

Total leukocyte enumeration was performed manually via hemocytometry according to Schalm et al. (1975). The operational principle dictates that erythrocytes are completely lysed by a specialized WBC diluting fluid, while the leukocytes remain intact with their nuclei stained a deep violet-black.

A precise 1:20 dilution of whole blood was prepared by drawing blood and WBC diluting fluid up to the appropriate markers in a standard WBC diluting pipette. The dilution was mixed thoroughly and charged onto a Neubauer hemocytometer counting chamber. The total number of leukocytes was counted across the 4 large primary corner squares of the grid using the low-power objective (x10) of a light microscope. The accumulated count was multiplied by a dilution factor of 50 to express the final total WBC count per microliter (µL) of blood.

Total Red Blood Cell (RBC) Count

Erythrocyte enumeration was performed manually using the manual hemocytometry method described by Schalm et al. (1975). The diluting fluid used is strictly isotonic and formulated with a high specific gravity to prevent the red blood cells from settling too rapidly during counting.

A 1:200 dilution of the anticoagulated whole blood was prepared using an RBC diluting pipette. The Neubauer hemocytometer counting chamber was carefully flooded with the fluid dilution. Erythrocyte counting was executed across 5 small squares within the central grid area with the aid of a manual counter under the high-power objective (40x) of a light microscope. The raw RBC count obtained from the 5 squares was multiplied by a calculation factor of 10,000 to express the final concentration as RBC count per milliliter (mL) of whole blood.

Statistical Analysis

All experimental data obtained from the growth parameters, manual hematological reports, and serum protein assays were expressed as the Mean ± Standard Deviation (SD). Statistical comparisons between the Control cohort and the malnourished cohort were evaluated using an independent Student's t-test. Differences between variable means were considered statistically significant at a confidence level of 95% *($p < 0.05$).* All statistical calculations were performed using the IBM SPSS Statistics software package (Version 23.0).

RESULTS AND DISCUSSION

Growth Performance and Body Weight Dynamics

The dietary administration of a low-protein, high-carbohydrate (3.47% protein) diet over the experimental period induced a profound, progressive depletion in the physical growth performance of the Wistar rats. As demonstrated in Table 4, there was no statistically significant difference in baseline body weights between the cohorts at the initial week (61.64 ± 4.08g vs. 60.58 ± 10.35g; *$t = 0.213$, $p = 0.837$*), confirming optimal baseline homogeneity.

Table 4: Weekly Changes in Body Weight (g) of Control and Malnourished Rats

Sampling Interval	Control Group mean	Malnourished Group Mean	*t-value*	*p-value*
Initial Week	61.64±4.08	60.58 ± 10.35	0.213	0.837
Week 1	79.16 ± 3.84	48.94± 9.77	6.234	< 0.001
Week 2	114.16 ± 12.48	45.18 ±7.50	10.605	< 0.001
Week 3	165.58 ± 29.90	42.14 ± 7.46	8.951	< 0.001
Week 4	222.26 ± 44.96	38.66 ± 5.23	9.071	< 0.001

However, by Week 1, the cohorts separated sharply. The control group displayed normal, sigmoidal mammalian developmental weight gain, escalating to a final weight of 222.26 ± 44.96g by Week 4. In stark contrast, the malnourished group exhibited an immediate and sustained failure to thrive, exhibiting severe somatic wasting that dropped their body mass to a final weight of 38.66 ± 5.23g *($t = 9.071$, $p < 0.001$)*.

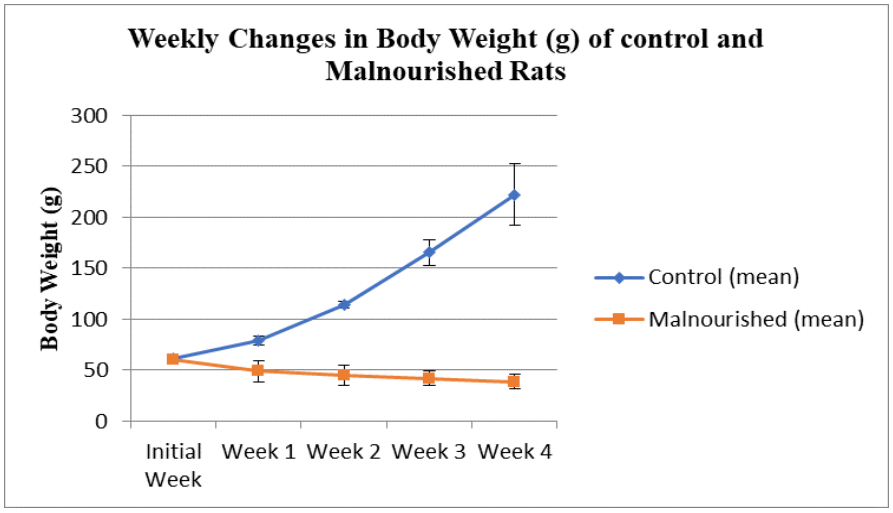

Figure 1: Weekly changes in body weight(g) of control and malnourished rats

This structural decline was accompanied by clear macro-morphological markers of advanced kwashiorkor-like pathology, including severe lethargy, reduced motor patterns, facial/paw edematous approximations, and extensive bilateral alopecia. The high standard deviations observed in the final weights of the control group reflect typical healthy developmental variations, whereas the narrow variance in the malnourished group highlights an absolute biological constraint imposed by severe macronutrient restriction. When dietary protein intake falls below the critical threshold required to maintain baseline metabolic machinery, the organism initiates a survival-driven catabolic cascade. Endogenous structural proteins—primarily from skeletal muscle tissue—are systematically degraded via proteolytic pathways to yield free amino acids for vital visceral synthesis and gluconeogenesis (Mhlomi et al., 2022; Waterlow, 1984).

Serum Protein Profiles and Hepatic Biosynthetic Shifts

The biochemical profiles of the circulating serum proteins provided deep evidence of severe visceral protein depletion (Table 5). Total protein concentrations collapsed from a baseline of 3.50 ± 0.66g/dL in the control group to 1.64 ± 0.55g/dL in the experimental group (*$t = 4.841$, $p = 0.001$*). This profound hypoproteinemia was driven by a parallel

breakdown in both the serum albumin fraction (2.14± 0.36g/dL reduced to 1.00 ± 0.30g/dL; *t = 5.440, p < 0.001*) and the total globulin fraction (1.36 ± 0.29g/dL reduced to 0.64 ± 0.26g/dL; *t = 4.133, p = 0.003*).

Table 5: Serum Protein, Albumin, and Globulin Profiles (g/dL)

Experimental Cohort	Total Protein	Albumin	Globulin
Control Group mean	3.50 ± 0.66	2.14 ± 0.36	1.36 ± 0.29
Malnourished Group mean	$1.64 ± 0.55	1.00 ± 0.30	0.64 ± 0.26
t-value	4.841	5.440	4.133
p-value	0.001	< 0.001	0.003

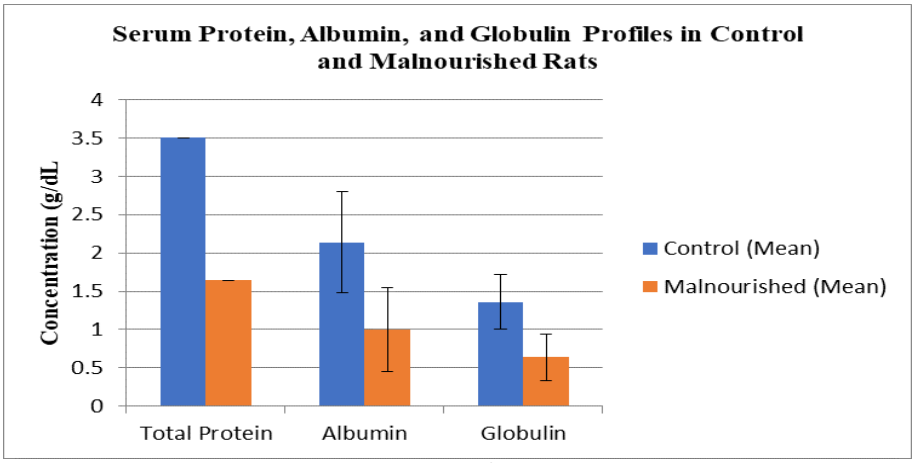

Figure 2: Serum protein, albumin and globulin profiles in control and malnourished rats

Mechanistically, this simultaneous drop across protein fractions reflects a major hepatic metabolic shift. Under conditions of severe amino acid scarcity, the liver fundamentally downregulates its translation machinery, dramatically suppressing the transcription and secretion of primary structural proteins like albumin (Sulyman & Ibrahim, 2024).

Interestingly, historical clinical literature focusing on infected, malnourished children frequently notes a "globulin sparing effect," where gamma-globulin levels remain artificially elevated or unchanged despite total body protein collapse due to active, secondary environmental infections (Suskind, et. al., 1976). However, because our study was executed within a highly controlled, uninfected laboratory environment, the globulin fraction dropped in unison with albumin. This underscores that in the absence of infectious confounders, true, uncomplicated protein deficiency results in a total systemic collapse of all major serum protein fractions.

Hematological Responses and Erythroid Collapse

The erythroid parameters detailed in Table 6 reveal a severe, classic manifestation of nutritional microcytic or normocytic anemia. Hematocrit (PCV) levels were effectively cut in half, dropping from 46.60 ± 1.20% in healthy controls to 24.40 ± 2.94% in the malnourished rats *(t = 15.632, p < 0.001)*. This was mirrored by a matching drop in blood hemoglobin concentration (15.48 ± 0.41g/dL to 7.86 ± 0.71g/dL; *t = 20.781, p < 0.001*) and absolute erythrocyte counts (10.21± 0.26 x 10^6mm^3 down to 5.96 ± 1.20 x 10^6mm^3; *t = 7.736, p = 0.001*).

Table 6: Hematological Profiles and Differential Leukocyte Counts

Parameter Measured	Control Group Mean	Malnourished Group Mean	*t-value*	*p-value*
Hematocrit / PCV (%)	46.60 ± 1.20	24.40 ± 2.94	15.632	< 0.001
Hemoglobin (g/dL)	15.48 ± 0.41	7.86 ± 0.71	20.781	< 0.001
Erythrocytes (10^6mm^3)	10.21 ± 0.26	5.96 ± 1.20	7.736	0.001
Leucocytes (10^3µL)	10.33 ± 0.36	6.68 ± 1.90	4.219	0.012
Lymphocytes (%)	56.80 ± 2.14	52.40 ± 2.06	3.312	0.011
Neutrophils (%)	43.20 ± 2.14	47.60 ± 2.06	-10.839	< 0.001

This extensive decline demonstrates that severe, prolonged dietary protein restriction simultaneously disrupts the oxygen-carrying capacity of the blood and cripples cell-mediated immune defense mechanisms (Müller & Krawinkel, 2005). The experimental group displayed a dramatic downward shift across all red blood cell parameters, indicating the development of a severe, hypoplastic nutritional anemia.

This profound erythroid collapse is directly tied to the suppression of erythropoietin (EPO) synthesis. Erythropoietin is a glycoprotein hormone heavily dependent on adequate hepatic and renal protein synthesis matrices. Due to the extreme lack of essential amino acids induced by the 3.47% protein diet, the biological cascade governing bone marrow erythropoiesis is severely halted. The body prioritizes its extremely scarce amino acid pool toward basic survival, suppressing red blood cell production and resulting in a synchronized drop in circulating blood metrics.

Leucocyte Dynamics and Immune Shifts

Evaluation of the circulating white blood cell profiles revealed a significant drop in total leukocyte counts, falling from 10.33 ± 0.36 x 10^3µL in controls to 6.68 ± 1.90 x 10^3µL in the experimental group *(t = 4.219, p = 0.012)*. The high

standard deviation (±1.90) seen in the malnourished cohort is a direct reflection of the small sample size *(n=5)*, which inherently increases variance.

The differential leukocyte count demonstrated a subtle but highly informative statistical shift. Relative lymphocyte percentages decreased from 56.80 ± 2.14% to 52.40 ± 2.06% ($t = 3.312$, $p = 0.011$), while relative neutrophil percentages rose complementarily from 43.20 ± 2.14% to 47.60 ± 2.06% *($t = -10.839$, $p < 0.001$)*.

This leukocyte profile points directly to severe nutritional leukopenia. The observed drop in relative lymphocytes is highly characteristic of malnutrition-induced thymic involution or lymphoid atrophy, where the primary lymphoid organs (the thymus and spleen) lose architectural integrity due to missing protein building blocks, drastically slowing down lymphocyte proliferation. Concurrently, the relative percentage increase in neutrophils must not be misinterpreted as true, absolute neutrophilia (which would indicate bacterial infection). Instead, as our controlled model was completely pathogen-free, this shift represents a relative percentage increase caused by a combination of profound lymphopenia and a chronic, systemic cortisol-driven stress response to severe metabolic starvation.

Reviewer Synthesis and Model Validation

Ultimately, these data strongly reaffirm the validity of the historical macronutrient thresholds defined by Boyd et al. (1968). By evaluating these targets against localized raw parameters—utilizing Garri as a primary carbohydrate base and ground soybean as a heavily restricted protein variable—this model successfully approximates the systemic, multilineage failures observed in human kwashiorkor.

While the compact sample size utilized remains an inherent limitation affecting broad generalizability, the highly unified, significant drops across physical, hepatic, erythroid, and leukocyte pathways demonstrate that this low-cost, manually reproducible model offers a robust laboratory framework for testing downstream therapeutic nutritional interventions.

CONCLUSION

In conclusion, this study demonstrates that maintaining young male Wistar rats on a low-protein, high-carbohydrate diet containing a strict 3.47% protein threshold induces severe, system-wide degradation. Over the extended observation period, this precise nutritional restriction led to severe somatic wasting, complete failure to thrive, and profound hypoproteinemia characterized by a parallel collapse of both serum albumin and globulin fractions. Furthermore, the diet triggered severe nutritional anemia alongside profound leukopenia and lymphopenia. Because these outcomes occurred within a highly controlled, pathogen-free environment, they offer a clear look at uncomplicated protein-energy malnutrition (PEM) independent of infectious or environmental confounders.

While these results provide a valuable multi-parameter baseline, important translational limitations must be acknowledged. Rodent metabolism operates at a significantly higher mass-specific basal rate than human metabolism, meaning the timeline and severity of tissue wasting observed in this animal model approximate rather than perfectly mirror the clinical progression of human kwashiorkor or marasmus.

Consequently, future research should build directly upon this baseline by introducing multi-tiered, dose-response studies with targeted leguminous or micro-nutritional dietary supplements to evaluate structural recovery. Additionally, longer-term longitudinal studies are needed to map the potential permanence of early-life systemic shock, combined with the evaluation of specific molecular and inflammatory markers—such as cytokine profiles or tissue-specific gene expressions—to clarify the cellular mechanics driving malnutrition-induced organ and marrow atrophy. Ultimately, this validated model serves as a reliable, accessible experimental framework necessary for designing and testing global public health and therapeutic nutritional interventions.

REFERENCES

Boyd, E. M., & Carsky, E. (1969). Kwashiorkorigenic diet and its metabolic effects in albino rats. *Acta Pharmacologica et Toxicologica*, *27*(4), 284–294. https://doi.org/10.1111/j.1600-0773.1969.tb01221.x

Boyd, E. M., Boulanger, M. A., & De Castro, E. S. (1968b). Phenacetin toxicity and dietary protein. *Pharmacological Research Communications*, *1*(1), 15–22.

Cuthbertson, W. F. J. (1957). Nutrient requirements of the laboratory rat. *Proceedings of the Nutrition Society*, *16*(1), 70–76. https://doi.org/10.1079/PNS19570017

Golden, M. H. (1998). The development of concepts of malnutrition. *The Journal of Nutrition*, *128*(2), 444S–450S. https://doi.org/10.1093/jn/128.2.444S

Maliza, R., Alimuddin, T., Santoso, P., Jannatan, R., & Zikrah, A.A., (2024). Effects of lima bean *(Phaeolus lunatus)* flour on cognitive function and growth recovery malnutrition rats. *J. Microbiol Biotech Fodd Sci, 13 (4) e 10332.* https://doi.org/10.55251/jmbfs.10332

Mhlomi, Y. N., Unuofin, J. O., Otunola, G. A., & Afolayan, A. J. (2022). Assessment of rats fed protein-deficient diets supplemented with *Moringa oleifera* leaf meal. *Current Research in Nutrition and Food Science Journal*, *10*(1), 45–55. https://doi.org/10.12944/crnfsj.10.1.04

Müller, O., & Krawinkel, M. (2005). Malnutrition and health in developing countries. *Canadian Medical Association Journal*, *173*(3), 279–286. https://doi.org/10.1503/cmaj.050342

Okediran, B.S., Amid, S.A.,, Sanusi, F. & Oladesu, K.O. (2021). Hematological and biochemical changes associated with male rats deprived of feed and water. *Ceylon Journal of Science 50(1), 11-16. http://doi.org/10.4038/cjs.v50i1.7842*

Patel, S., Kotadiya, A., Patel, S., Shrimali, B., Joshi, N., et al. (2024). Age-related changes in hematological and biochemical profiles of healthy Wistar rats. *Laboratory Animal Research*, *40*(1), 12–21. https://doi.org/10.1186/s42826-024-00194-7

Rippon, W. P. (1959). The reproduction of kwashiorkor in the albino rat with commercial food components. *British Journal of Nutrition*, *13*(2), 241–249. https://doi.org/10.1079/BJN19590033

Schalm, O. W., Jain, N. C., & Carroll, E. J. (1975). *Veterinary Hematology* (3rd ed.). Lea & Febiger.

Sulyman, R. A., & Ibrahim, F. (2024). Ameliorative potentials of leguminous diet interventions on total protein and lipid profiles of protein-energy malnourished Wistar rats. *FUDMA Journal of Sciences*, *8*(3), 204–211. https://doi.org/10.47430/fjs.2024.0803.14

Suskind, R., Sirishinha, S., Vithayasai, V., Edelman, R., Damrongsak, D., Charupatana, C., and Olsan, R. (1976). Immunoglobulins and antibody response in children with protein-calorie malnutrition. *The American Journal of Clinical Nutrition, 29, 836-841.*

Waterlow, J. C. (1984). The rate of protein turnover in the whole body in relation to growth and malnutrition. *Clinical Science*, *67*(5), 465–472. https://doi.org/10.1042/cs0670465